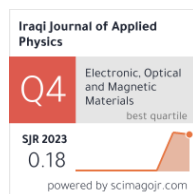


Ibrahim M. Jasim
Arshad Hmood

Microelectronics and
Nanotechnology
Research Laboratory
(M. N. R. Lab.),
Department of Physics,
College of Science,
University of Basrah,
Basrah, IRAQ



A Rapid and Efficient Preparation of Thermoelectric Zintl Antimonites $\text{YbZn}_{2-x}\text{Mn}_x\text{Sb}_2$ by Microwave Irradiation Solid State Technique

This work addresses a synthesis of Zintl antimonite compounds $\text{YbZn}_{2-x}\text{Mn}_x\text{Sb}_2$ ($0.0 \leq x \leq 2.0$) using a microwave-assisted solid state technique. The technique involves utilizing an active carbon as a susceptor around the primary components to produce large compact ingots. The microwave assisted solid state synthesis offers considerable advantages such as acceleration the reactions induced by high heating surrounding susceptor of starting components and gives large quaternary ingots in shorter time about 10 minutes compared with other traditional methods. Thermoelectric characterizations were measured for all synthesized compounds and among them, the compound $\text{YbZn}_{1.6}\text{Mn}_{0.4}\text{Sb}_2$ is found to be best one as it shows Seebeck coefficient of $-53.04 \mu\text{V/K}$, and power factor of $1.78 \mu\text{W/cm.K}^2$ at 523 K with carrier concentration of $4.8 \times 10^{21} \text{ cm}^{-3}$ at 300K.

Keywords: Thermoelectricity; Zintl antimonite; Microwave synthesis; Active carbon
Received: 29 May 2024; Revised: 23 July 2024; Accepted: 30 July 2024

1. Introduction

Recent articles into thermoelectric materials (TEMs) have focused on studying heat and electricity as they can be converted to each other by their devices [1-4]. The efficient TEMs can offer high electrical conductivity, Seebeck coefficient, and low thermal conductivity. The efficiency of conversion is based on the dimensionless thermoelectric figure of merit (ZT) as:

$$ZT = \left(\frac{S^2 \sigma}{K} \right) T \quad (1)$$

where S , σ , K , and T are Seebeck coefficient, electrical conductivity, thermal conductivity, and absolute temperature, respectively [5-8]

Beside above, TEMs would provide small-band gap since it can be expressed by the relation $E_g = 2eS_{\max}T_{\max}$ and a range of carrier concentration of 10^{19} - 10^{21} cm^{-3} [2,9]. Changing the chemical compositions or forming solid solutions is often used to adjust the carrier concentrations, mobility, effective mass, and lattice thermal conductivity [2] thus the compounds YbZn_2Sb_2 and YbMn_2Sb_2 are considered as important TEMs. The power factor ($S^2\sigma$) is considered as a vital part of studying of TEMs. Recently, many studies have been focused on developing or exploring TEMs with high values of $S^2\sigma$ and low thermal conductivity [10,11]. These materials could exhibit small band gaps and suitable carrier concentrations, making it superior toward metals [12]. The presence of heavy atoms, large unit cells, and complex structures contribute to enhance their efficient thermoelectric properties. Previous methods for synthesizing Zintl phase compounds required extended heating periods, whereas microwave-assisted solid state technique emerged to be an efficient synthetic method within a rapid time

(10 mins). Thermoelectric Zintl phase of compounds have been prepared by direct solid state technique and found taking a long time under heating for example: $\text{YbZn}_{2-x}\text{Mn}_x\text{Sb}_2$ was synthesized at 1323K for 30 hours and subsequent annealing for 30 hours [13], $\text{BaMn}_{2-x}\text{Zn}_x\text{Sb}_2$ was obtained at 1373K with a rate of 600 K/h, then held at 1373K for 1 hour [14]. The other examples include YbZn_2Sb_2 at 1323K for 30 hours [15], $\text{Ca}_{1-x}\text{Yb}_x\text{Zn}_2\text{Sb}_2$ at 1273K for 48 hours [16], $\text{YbCd}_{2-x}\text{Mg}_x\text{Sb}_2$ at 1273K for 72 hours [17], SrZn_2Sb_2 at 1073K for 5 days [18], $\text{Ca}_{1-x}\text{Eu}_x\text{Zn}_2\text{Sb}_2$ at 1273K for 3 days [19], $\text{Yb}_x\text{Eu}_{1-x}\text{Cd}_2\text{Sb}_2$ at 1473K for 24 hours [20]. In our work, the Zintl antimonite compounds $\text{YbZn}_{2-x}\text{Mn}_x\text{Sb}_2$ with ($x=0.0, 0.4, 0.8, 1.2, 1.6, 2.0$) are synthesized in short time (10 min) under microwave irradiation proves to be an efficient this method, allows materials to reach high temperatures without causing electric discharges. The work also focuses on modification of cation percentages of Zn-Mn in $\text{YbZn}_{2-x}\text{Mn}_x\text{Sb}_2$ ingots ($x=0.0, 0.4, 0.8, 1.2, 1.6$, and 2.0) using microwave-assisted solid state synthesis, demonstrate their potential for thermoelectric applications. Reportedly, antimony-based Zintl compounds exhibit unique structural characteristics which lead to low lattice thermal conductivity at high temperatures. Many articles have recommended to use of microwave-assisted solid state as an efficient technique which is employed to prepare Zintl phase compounds $\text{YbZn}_{2-x}\text{Mn}_x\text{Sb}_2$ with promising thermoelectric applications [12]. Importantly, a microwave-assisted solid state provides high energy, easy work up and eco-friendly methodology than other traditional techniques [21]. Thus, a successful modification in the percentage of cations of Zn-Mn in $\text{YbZn}_{2-x}\text{Mn}_x\text{Sb}_2$ ingots ($x=0.0$,

0.4, 0.8, 1.2, 1.6, 2.0) under microwave-assisted solid state synthesis is reported. Meanwhile, antimony (Sb)-based Zintl antimonites have been demonstrated to behave as an efficient thermoelectric material possessing electric crystal, and photonic glass nature. Their unique crystal structure emerges in low lattice thermal conductivity at high temperature [22].

2. Experimental Part

Highly-pure (>99.99%, 200 meshes) elements (Yb, Zn, Mn, and Sb) were ordered from Sigma-Aldrich. By microwave-assisted solid state technique, the Zintl antimonite compounds $\text{YbZn}_{2-x}\text{Mn}_x\text{Sb}_2$ were prepared from 2 g of each powder, and mixed by an agate mortar at a period 20 mins to obtain a homogenous mixture. This mixing is necessary to make sure a complete homogenous mixture. The stoichiometric ratio of $\text{YbZn}_{2-x}\text{Mn}_x\text{Sb}_2$ were performed according to ($x = 0.0, 0.4, 0.8, 1.2, 1.6$ and 2.0). This mixture was batched and taken inside a clean quartz ampoule (20cm long and 1cm in diameter) with sealed under high vacuum of 10^{-5} mbar. An active carbon (susceptor) was surrounded the quartz ampoule by alumina crucible (7cm high and 5cm in diameter), to absorb microwave irradiation and initiate heating under a microwave-assisted solid state with microwave power of 1000W. The active carbon also helps to raise reaction temperature to be reached 1123K for 10 min (2 min ON: 2 min OFF) and the temperature of ampoule was controlled using an infrared thermometer (S-CA-1168) as shown in Fig. (1).

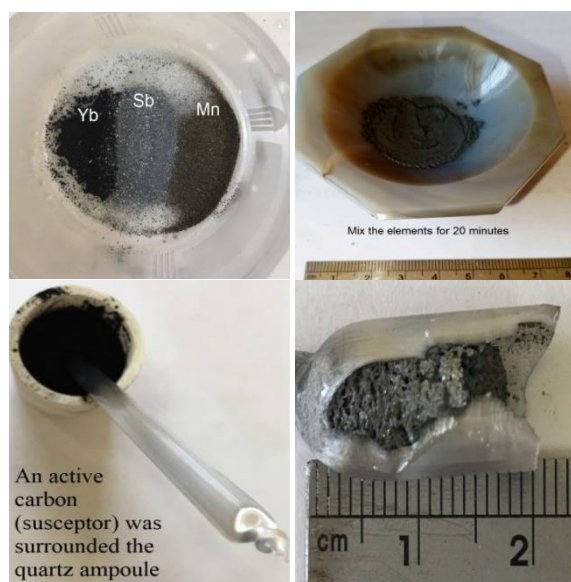


Fig. (1) Schematic representation of $\text{YbZn}_{2-x}\text{Mn}_x\text{Sb}_2$ compounds by microwave assisted solid state technique

The ampoule was further cooled to room temperature to produce ingot. The structural analysis, thermoelectric characterizations, and morphological study of the resulted ingots are reported. The ingots $\text{YbZn}_{2-x}\text{Mn}_x\text{Sb}_2$ ($0.0 \leq x \leq 2.0$) were ground into fine

powders which pressed into disk shapes with dimensions ($\phi 10\text{mm} \times 0.5\text{mm}$) under cold pressing at 10 ton. The Seebeck coefficient (S) of polished disks was measured by calculated the slope of the linear relationship between the thermoelectromotive force and the temperature difference between the two ends of each sample, as mentioned in previous reference [21]. The four-point probe method was using to measure the electrical conductivity (σ) in a vacuum at 10^{-3} mbar at a temperature range of 298-523K. The carrier concentration (n) was determined at room temperature from the Hall voltage measurement by applying magnetic field of 1 T using a PHYWE 6480 electromagnetic.

3. Results and Discussion

Figure (2) shows the x-ray diffraction (XRD) patterns for $\text{YbZn}_{2-x}\text{Mn}_x\text{Sb}_2$ structures ($0.0 \leq x \leq 2.0$), which are indexed as hexagonal structure according to JCPDS cards 98-041-9689 and 01-083-1684. The dominant diffraction peaks of the synthesized compounds were indexed as hexagonal structures, which confirm the polycrystalline structure of the $\text{YbZn}_{2-x}\text{Mn}_x\text{Sb}_2$ sample. The obtained results proved the high efficiency of the use of a microwave-assisted solid state as a synthetic technique in addition under very short time without annealing process.

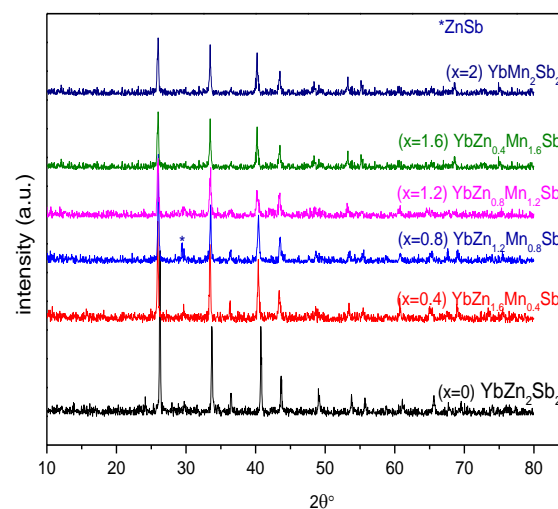


Fig. (2) XRD patterns of $\text{YbZn}_{2-x}\text{Mn}_x\text{Sb}_2$ powders

The scanning electron microscopy (SEM) images are shown in Fig. (3) for the prepared compounds $\text{YbZn}_{2-x}\text{Mn}_x\text{Sb}_2$ ($x = 0.0, 0.4, 0.8, 1.2, 1.6, 2.0$), meanwhile, the particles were emerged under irradiation process to configure the nanoparticle structures on the surface of ingots. The nanoparticles were noticed as they appeared in non-uniformly distributed over the surface as seen in the Fig. (4). The SEM morphologies show the appearance of crystallite particles due to the effect of modification in Zn-Mn moiety observed in the doping.

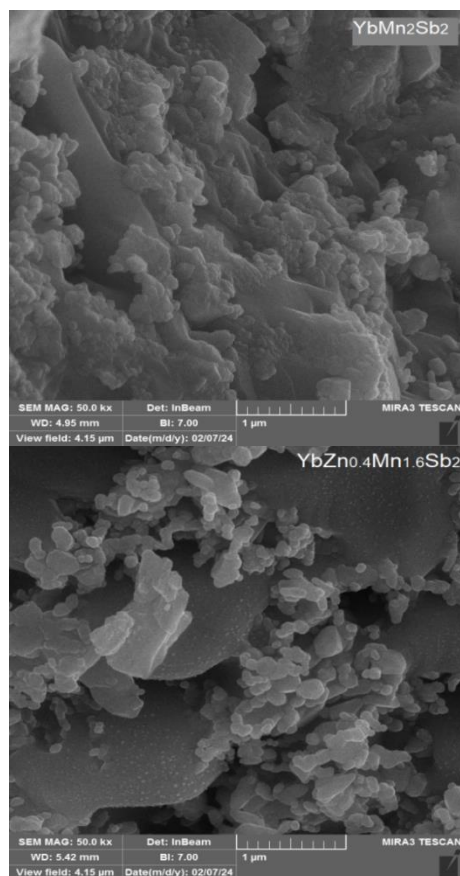
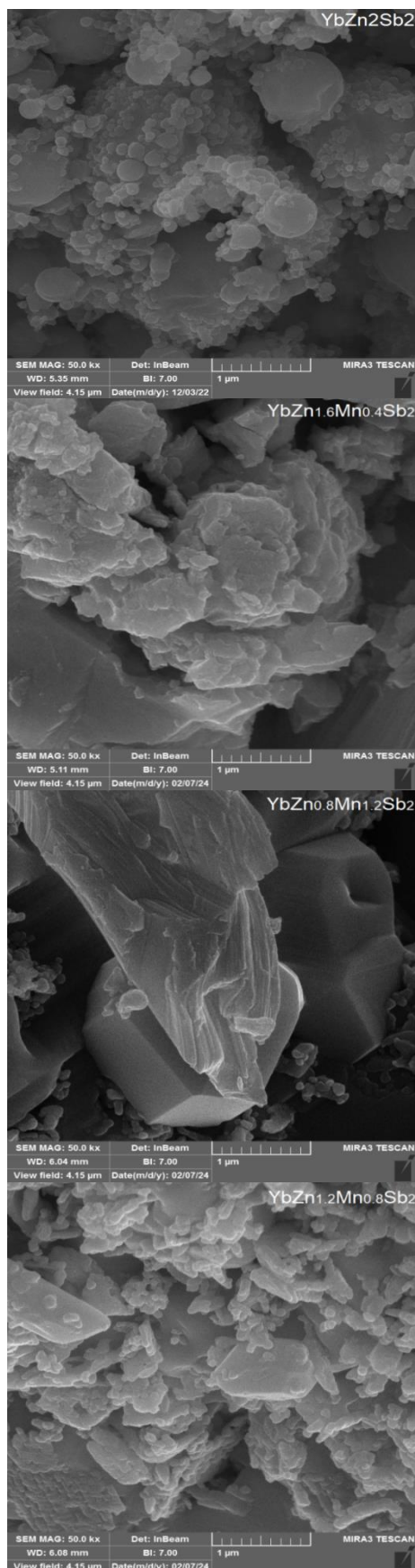
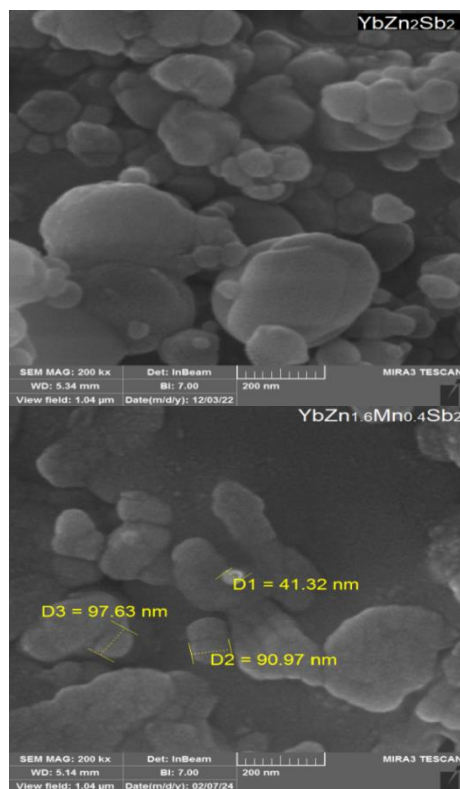


Fig. (3) SEM images of $\text{YbZn}_{2-x}\text{Mn}_x\text{Sb}_2$ ingots when $(0.0 \leq x \leq 2.0)$ with micro-scale of $1\mu\text{m}$



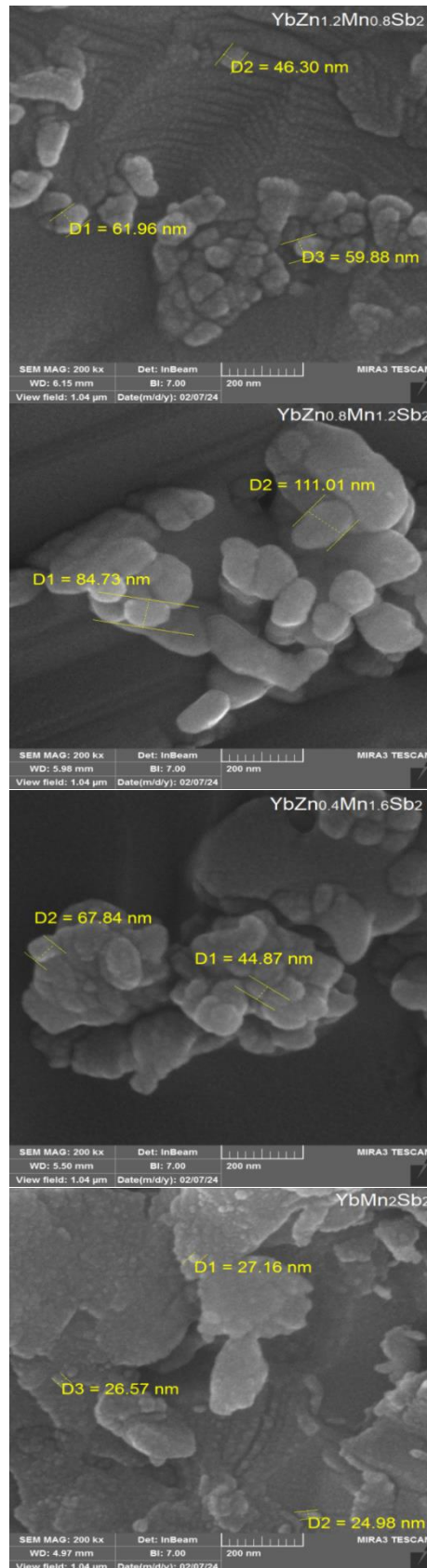


Fig. (4) SEM images of $\text{YbZn}_{2-x}\text{Mn}_x\text{Sb}_2$ ingots when $(0.0 \leq x \leq 2.0)$ with nano-scale 200nm

The electrical conductivity (σ) of the samples increased when the temperature was increased and

this behavior is in agreement with non-degenerate semiconductor behavior of compositions for all value of x specially for two values (0.4 and 1.2) and this makes it the most promising prepared of the materials in this work as thermoelectric materials. This improvement is very clear according to the value $x=0.4$ which showed high electrical conductivity (σ) where values of $6.5 \times 10^4 \text{ S/m}$ as shown in Fig. (5). It is noticeable from this figure that doping with a small percentage of Mn gave the best result of σ . By using ($\sigma = ne\mu$) and ($R_H = 1/ne$) the Hall mobility and Hall coefficient are calculated, respectively. The carriers concentration (n) calculated by Hall voltage and other parameters are listed in table (1). The Hall coefficient (R_H) of compound $\text{YbZn}_{1.6}\text{Mn}_{0.4}\text{Sb}_2$ is $-1.28 \times 10^{-9} \text{ m}^3/\text{C}$ and Hall mobility is $31.90 \text{ cm}^2/\text{V.s}$ and the carriers concentration (n) is $-4.8 \times 10^{21} \text{ cm}^{-3}$.

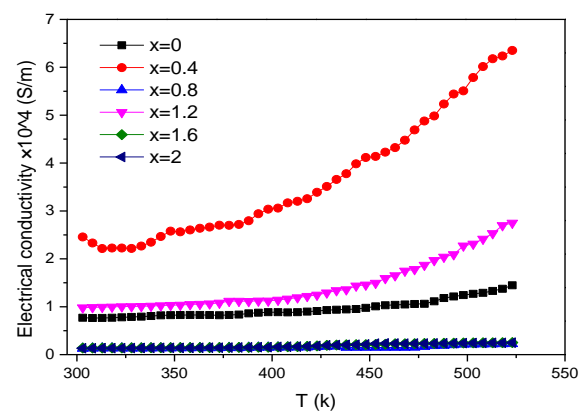


Fig. (5) Electrical conductivity as a function of temperature of $\text{YbZn}_{2-x}\text{Mn}_x\text{Sb}_2$ when $(0.0 \leq x \leq 2.0)$

Table (1) Electrical conductivity (σ), Seebeck coefficient (S), Power factor ($S^2\sigma$), Hall coefficient (R_H), Hole concentration (p), Hall mobility (μ), Lattice constants (a, c)

x	$\sigma \times 10^4$ (S/m)	S ($\mu\text{V/K}$)	$S^2\sigma$ ($\mu\text{W/cm.K}^2$)	$R_H \times 10^{-9}$ (m^3/C)	$n \times 10^{21}$ (cm^{-3})	μ ($\text{cm}^2/\text{V.s}$)
0.0	0.77	38.90	0.15	0.7	$P=8.12$	5.92
0.4	2.45	-30.36	0.23	-1.28	-4.8	31.90
0.8	0.12	-21.70	0.06	-0.26	-23.9	0.313
1.2	0.98	-6.10	0.003	-0.48	-12.9	4.74
1.6	0.13	-14.80	0.003	-2.23	-2.7	3.00
2.0	0.13	-10.50	0.001	-10.16	-0.6	13.45

Figure (6) shows the temperature dependency of the Seebeck coefficient for $\text{YbZn}_{2-x}\text{Mn}_x\text{Sb}_2$ ($0.0 \leq x \leq 2.0$). The measured values of Seebeck coefficient for five samples are a negative value n-type conductivities which means that the majority of carriers are electrons, while the compound YbZn_2Sb_2 (when $x=0$) is p-type as the holes which are represented the majority of carriers of electrical transports. The Seebeck coefficient increased when Mn-doping was decreased. In addition, the highest calculated value of the Seebeck coefficient was obtained when the doping level $x=0.4$ was $-53.04 \mu\text{V/K}$ at 523K. The Seebeck coefficient of non-degenerated semiconductor can be described using the following equation [23]:

$$S = \frac{8\pi^2 k_B^2}{3eh^2} m^* T \left(\frac{\pi}{3n} \right)^{2/3} \quad (1)$$

where k_B is Boltzmann's constant, h is Plank constant, and m^* is the effective mass

The above relationship shows that Seebeck coefficient is highly dependent on electrical conductivity. Therefore, an rising in the Seebeck coefficient values could be attributed to rising of levels in donor state, and these values increased with the chosen Zintl compounds that have high values of m^* .

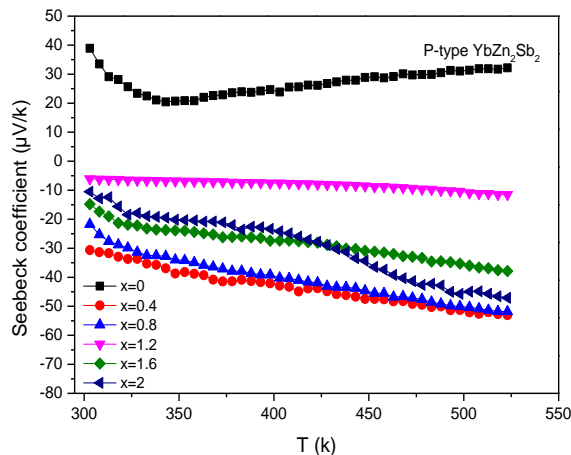


Fig. (6) Seebeck coefficient as a function of temperature of $\text{YbZn}_{2-x}\text{Mn}_x\text{Sb}_2$ when $(0.0 \leq x \leq 2.0)$

The temperature dependency of the power factor ($S^2\sigma$) of Zintl compounds $\text{YbZn}_{2-x}\text{Mn}_x\text{Sb}_2$ ($0.0 \leq x \leq 2.0$) under microwave assisted solid state is 523K as shown in Fig. (7). The highest calculated value of power factor ($S^2\sigma$) for the prepared sample $\text{YbZn}_{1.6}\text{Mn}_{0.4}\text{Sb}_2$ equals to $1.78 \mu\text{W}/\text{cm}\cdot\text{K}^2$ at 523 K.

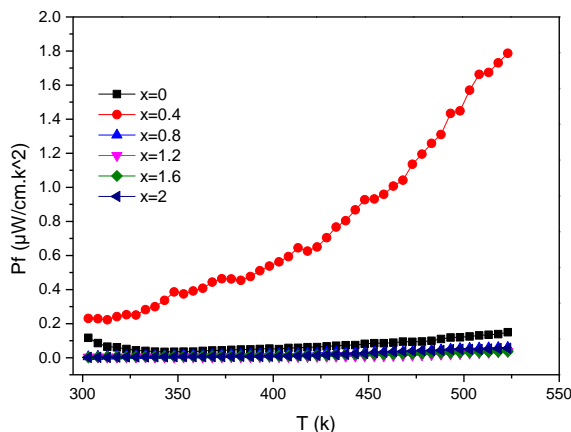


Fig. (7) Power factor as a function of temperature of $\text{YbZn}_{2-x}\text{Mn}_x\text{Sb}_2$ when $(0.0 \leq x \leq 2.0)$

4. Conclusions

In concluding remarks, $\text{YbZn}_{2-x}\text{Mn}_x\text{Sb}_2$ ($0.0 \leq x \leq 2.0$) Zintl compounds were successfully prepared using microwave-assisted solid state at 1123K for short time (10 min) and the pure phase was obtained for the same time without any additional time for annealing. The prepared compounds have pure phase with hexagonal structure. The

$\text{YbZn}_{1.6}\text{Mn}_{0.4}\text{Sb}_2$ sample showed moderate electrical conductivity and a higher Seebeck coefficient with higher power factor of $1.78 \mu\text{W}/\text{cm}\cdot\text{K}^2$ at 523K than those samples reported elsewhere.

Acknowledgement

The authors express their gratitude for the support received from the Department of Physics, College of Science, University of Basrah, Iraq.

References

- [1] G.S. Nolas, J. Sharp and H.J. Goldsmid, "Thermoelectrics Basic Principles and New Materials Developments", Springer Heidelberg (NY, 2001), Ch. 3, pp. 72-73.
- [2] L. Chen, R. Liu and X. Shi, "Thermoelectric Materials and Devices", Elsevier (China, 2021), Ch.1, p. 2.
- [3] Y.X. Gan, "Nanomaterials for Thermoelectric Devices", Stanford (2018), Ch. 1, p. 3.
- [4] W. He et al., "Recent development and application of thermoelectric generator and cooler", *Appl. Energy*, 143 (2015) 1-25.
- [5] X. Du et al., "Enhanced thermoelectric performance of n-type Bi_2S_3 with added ZnO for power generation", *RSC Adv.*, 5 (2015) 1-12.
- [6] A. Kadhim, A. Hmood and H. Abu Hassan, "Electrical characterization of thermoelectric generators based on p-type $\text{Bi}_{0.4}\text{Sb}_{1.6}\text{Se}_{2.4}\text{Te}_{0.6}$ and n-type $\text{Bi}_2\text{Se}_{0.6}\text{Te}_{2.4}$ bulk thermoelectric materials", *Mater. Lett.*, 97 (2013) 24-26.
- [7] M.W. Gaultois et al., "Data-Driven Review of Thermoelectric Materials: Performance and Resource Considerations", *Chem. Mater.*, 25 (2013) 2911-2920.
- [8] A. Kadhim, A. Hmood and H. Abu Hassan, "Significant Influences of Selenium on the Electrical Properties of Bi_2Te_3 Compounds Synthesized Using Solid-State Microwave Irradiation", *Adv. Mater. Res.*, 501 (2012) 126-128.
- [9] A. Hmood, A. Kadhim and H. Abu Hassan, "Structural, characterization and electrical properties of $\text{AgPb}_m\text{Te}_{m-2}$ compounds synthesized through a solid-state microwave technique", *J. Hydro. Energy*, 41 (2016) 5048-5056.
- [10] N. Ghazi and A. Kadhim, "Thermoelectric properties of solid state reaction-prepared ZnO based alloys with various CuO doping in $(\text{CuO})_x(\text{ZnO})_{1-x}$ ", *Solid State Commun.*, 361 (2023) 115058.
- [11] X. Zhang et al., "Enhanced thermoelectric properties of $\text{YbZn}_2\text{Sb}_{2-x}\text{Bi}_x$ through a synergistic effect via Bi-doping", *Chem. Eng.*, 374 (2019) 589-595.
- [12] I. Nandhakumar, N.M. White and S. Beeby, "Thermoelectric Materials and Devices (Energy and Environmental Series", vol. 17,

- 1st ed., Royal Society of Chemistry, (UK, 2017), Ch. 1, p. 17.
- [13] T.J. Zhu et al., "Thermoelectric Properties of Zintl Compound YbZn_2Sb_2 with Mn Substitution in Anionic Framework", *J. Electron. Mater.*, 38 (2009) 1068-1071.
- [14] H.F. Wang, K.F. Cai and S. Chen, "Preparation and thermoelectric properties of $\text{BaMn}_{2-x}\text{Zn}_x\text{Sb}_2$ zintl compounds", *J. Mater. Sci.: Mater. Electron.*, 23 (2012) 2289-2292.
- [15] X. Zhang et al., "Spontaneously promoted carrier mobility and strengthened phonon scattering in p-type YbZn_2Sb_2 via a nano compositing approach", *J. Nano Energy*, 43 (2018) 159-167.
- [16] F. Gascoin et al., "Zintl Phases as Thermoelectric Materials: Tuned Transport Properties of the Compounds $\text{Ca}_x\text{Yb}_{1-x}\text{Zn}_2\text{Sb}_2$ ", *Adv. Func. Mater.*, 15 (2005) 203-206.
- [17] Q. Cao et al., "Thermoelectric properties of YbCd_2Sb_2 doped by Mg", *J. Alloys Comp.*, 680 (2016) 278-282.
- [18] H. Zhang et al., "Thermoelectric Properties of Polycrystalline SrZn_2Sb_2 Prepared by Spark Plasma Sintering", *J. Electron. Mater.*, 39 (2010) 1772-1779.
- [19] T.A. Wubienh et al., "Thermoelectric Properties of Zintl Phase Compounds of $\text{Ca}_{1-x}\text{Eu}_x\text{Zn}_2\text{Sb}_2$ ($0 \leq x \leq 1$)", *J. Electron. Mater.*, 45 (2016) 1233-1237.
- [20] H. Zhang et al., "Thermoelectric properties of $\text{Eu}_x\text{Yb}_{1-x}\text{Zn}_2\text{Sb}_2$ ", *J. Chem. Phys.*, 133 (2010) 204-209.
- [21] A. Kadhim, A. Hmood and H. Abu Hassan, "Preparation of $\text{Bi}_{0.4}\text{Sb}_{1.6}\text{Se}_{3x}\text{Te}_{3(1-x)}$ hexagonal rods and effect of Se on structure and electrical property", *J. Solid State Sci.*, 21 (2013) 110-115.
- [22] W. Zhao et al., "Enhanced thermoelectric performance via randomly arranged nanopores: Excellent transport properties of YbZn_2Sb_2 nanoporous materials", *J. Acta Materialia*, 60 (2012) 1741-1746.
- [23] K. Guo et al., "Enhanced Thermoelectric Figure of Merit of Zintl Phase $\text{YbCd}_{2-x}\text{Mn}_x\text{Sb}_2$ by Chemical Substitution", *Euro. J. Inorg. Chem.*, 26 (2011) 4043-4048.